JOURNAL OF GUIDANCE, CONTROL, AND DYNAMICS
Vol. 17, No. 1, January–February 1994

Model Reduction Methodology for Articulated, Multiflexible Body Structures

Allan Y. Lee* and Walter S. Tsuha†
Jet Propulsion Laboratory, California Institute of Technology, Pasadena, California 91009

Multibody dynamics simulation packages such as DISCOS are commonly used to simulate and analyze systems of interconnected rigid or flexible bodies. In many applications using these codes, the flexible components must be described in a way that when they are assembled, important system-level modes are accurately captured. The projection and assembly model reduction method, developed at the Jet Propulsion Laboratory, serves this purpose very well. However, early application of the method on the Galileo spacecraft model indicated mismatches in transfer function zeros between the full-order model and a reduced-order model constructed using the projection and assembly method. In this paper, an enhanced projection and assembly method, employing static correction modes to augment either the selected mode set of the system or the projected mode sets of the components is presented. The effectiveness of the proposed methodology in generating reduced-order system models, accurate at multiple system configurations and over a frequency range of interest, has been successfully demonstrated on a high-order finite element model of the Galileo spacecraft.

Background and Motivation

TO simulate and analyze the dynamical motion of articulated, multiflexible body structures, one can use multibody simulation packages such as DISCOS.[1] To this end, one must supply appropriate models for all the flexible components involved. For complex systems such as the Galileo spacecraft, practical considerations (e.g., simulation time) impose limits on the number of modes that each flexible body can retain in a given simulation. Reduced-order models of the system's flexible components are hence needed.

Model reduction methodologies are typically used to reduce a "large" system model to one that is "small" enough to facilitate analysis and control design, yet "rich" enough that it retains the salient features of the original system model. Although the literature on model reduction is vast, works that address the model reduction needs of articulated, multiflexible body structures are sparse and have only appeared recently.[2-5] Here, what is needed is a way of generating reduced-order component models that, when reassembled, produce a reduced-order system model that retains the salient features of the input-to-output mapping of the full-order system. The balanced component mode synthesis[2] and the projection and assembly[3,4] methodologies are two ways of performing this task.

The projection and assembly method has been intensively studied in recent years.[3,4,5] In this method, modes that contribute significantly to the system's input-to-output mapping are selected and are then "projected" onto the components. When the resultant reduced-order component models are reassembled, a reduced-order system model is obtained that exactly captures the selected system modes.[3,5] However, we observed a few drawbacks of this methodology when it was applied on a high-order Galileo model. In addition to the expected appearances of the unwanted extraneous modes,[3,5] mismatches in transfer function zeros between the full- and reduced-order system models were also unacceptably large. An enhanced projection and assembly method was proposed in Ref. 6 to address this zero mismatch problem. It employed static correction modes to augment the selected system mode set before the enlarged mode set was projected onto the component models. The effectiveness of the enhanced methodology in alleviating the zero mismatch problem was successfully demonstrated on a high-order finite element model of the Galileo spacecraft.[6]

This paper addresses the model reduction needs of articulated, multi-flexible body structures. Since the set of dominant system modes changes with system configurations in these structures, a composite mode set, consisting of "important" system modes from all system configurations of interest and not just from one particular system configuration, can be used to advantage. Again, this composite mode set is augmented with static correction modes. The effectiveness of the proposed methodology will be validated using a high-order, finite element model of the Galileo spacecraft.

Projection and Assembly Methodology Revisited[3-5]

The projection and assembly (P&A) method, as described in Refs. 3–5 is briefly reviewed here. To this end, consider the Galileo model depicted in Fig. 1. The system can be considered as the "sum" of two flexible components and a rigid body. The rotor may be rotated with respect to the stator using an

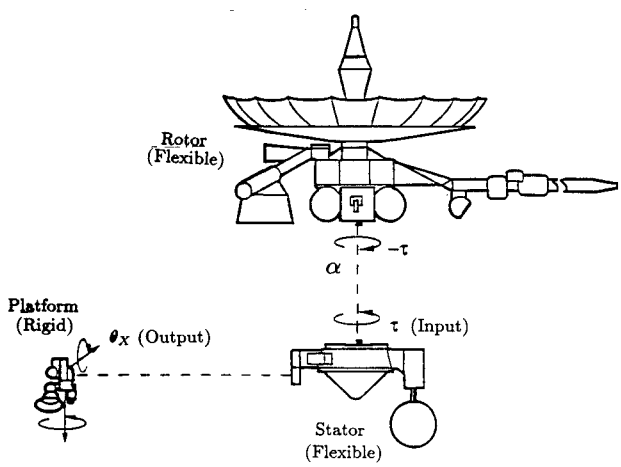

Fig. 1 Three-body topology of the Galileo Spacecraft Model.

Received April 13, 1992; revision received April 2, 1993; accepted for publication April 8, 1993.

*Member of Technical Staff, Guidance and Control Section, M.S. 198-326, 4800 Oak Grove Drive.

†Member of Technical Staff, Applied Technologies Section, M.S. 157-410, 4800 Oak Grove Drive.

actuator located at their interface. The relative orientation of the rotor with respect to the stator is denoted by a clock angle α (see Fig. 1). The undamped motion of component A (rotor) is described by

$$M^A_{pp}\ddot{x}^A_p + K^A_{pp}x^A_p = G^A_{pa}u^A_a$$
$$y^A_b = H^A_{bp}x^A_p \tag{1}$$

where x^A_p is a $p \times 1$ displacement vector, and M^A_{pp} and K^A_{pp} are $p \times p$ mass and stiffness matrices, respectively. Note that the matrix dimensions are indicated by its subscripts. The control distribution matrix G^A_{pa} is a $p \times a$ matrix, where a is the number of control input points. The output distribution matrix H^A_{bp} is a $b \times p$ matrix, where b is the number of outputs. Similar equations can also be written for component B (stator)

$$M^B_{qq}\ddot{x}^B_q + K^B_{qq}x^B_q = G^B_{qa}u^B_a$$
$$y^B_l = H^B_{lq}x^B_q \tag{2}$$

where the number of degrees-of-freedom (DOFs) of component B is q.

The system equations of motion at an articulation angle α can be constructed using the component equations and enforcing displacement compatibility at the component interface (I/F). To this end, let $P(\alpha) = [P^{A^T}_{pn}(\alpha), P^{B^T}_{pn}(\alpha)]^T$ be a full-rank matrix mapping a minimal system state x_n into

$$\begin{bmatrix} x^A_p \\ x^B_q \end{bmatrix} = \begin{bmatrix} P^A_{pn}(\alpha) \\ P^B_{qn}(\alpha) \end{bmatrix} [x_n] \tag{3}$$

where x_n is a $n \times 1$ vector. Here, $n = p + q - i$, i being the number of constraints. One way of generating the $P(\alpha)$ matrix will be described in the sequel [cf., Eqs. (11) and (12)]. For ease of notation, the dependencies of the matrices P^A_{pn}, P^B_{qn}, etc., on α are dropped in the sequel. Substituting $x^A_p = P^A_{pn}x_n$ and $x^B_q = P^B_{qn}x_n$ into Eqs. (1) and (2), premultiplying the resultant equations by $P^{A^T}_{pn}$ and $P^{B^T}_{qn}$, respectively, and summing the resultant equations give

$$M_{nn}\ddot{x}_n + K_{nn}x_n = G_{na}u_a$$
$$y_m = H_{mn}x_n \tag{4}$$

where

$$M_{nn} = P^{A^T}_{pn}M^A_{pp}P^A_{pn} + P^{B^T}_{qn}M^B_{qq}P^B_{qn}$$
$$K_{nn} = P^{A^T}_{pn}K^A_{pp}P^A_{pn} + P^{B^T}_{qn}K^B_{qq}P^B_{qn}$$
$$G_{na} = P^{A^T}_{pn}G^A_{pa} + P^{B^T}_{qn}G^B_{qa}$$
$$H_{mn} = [P^{A^T}_{pn}H^{A^T}_{bp}, P^{B^T}_{qn}H^{B^T}_{lq}]^T$$

Here $y_m = [y^{A^T}_b\ y^{B^T}_l]^T$, and $m = b + l$. To arrive at the equation for G_{na}, we have assumed that $u^A_a = u^B_a = u_a$. Otherwise, $G_{na}u_a$ in Eq. (4) should be replaced by $[P^{A^T}_{pn}G^A_{pa}, P^{B^T}_{qn}G^B_{qa}]$ $[u^{A^T}_a, u^{B^T}_a]^T$.

Let $(\Phi_{nn}, \Lambda_{nn}) = \text{eig}(K_{nn}, M_{nn})$, the "modal" equivalence of Eq. (4) is

$$I_{nn}\ddot{\xi}_n + \Lambda_{nn}\xi_n = \bar{G}_{na}u_a$$
$$y_m = \bar{H}_{mn}\xi_n \tag{5}$$

where ξ_n is the modal coordinates, i.e., $x_n = \Phi_{nn}\xi_n$. Also, $\Phi^T_{nn}M_{nn}\Phi_{nn} = I_{nn}$, $\bar{H}_{mn} = H_{mn}\Phi_{nn}$, $\bar{G}_{na} = \Phi^T_{nn}G_{na}$, and $\Lambda_{nn} = \Phi^T_{nn}K_{nn}\Phi_{nn}$ is a diagonal matrix with the undamped system eigenvalues along its diagonal.

In the P&A method,[3-5] only k of the system's n modes are kept, and the remaining $t(= n - k)$ modes are removed. That is

$$x_n = [\Phi_{nk} \quad \Phi_{nt}]\begin{bmatrix} \xi_k \\ \xi_t \end{bmatrix} \doteq \Phi_{nk}\xi_k \tag{6}$$

where ξ_k and ξ_t are generalized coordinates associated with the "kept" and "truncated" modes, respectively. Ways to select important system's modes that make a significant contribution to the system's input-to-output mapping have been suggested. See, e.g., the "balanced" realization approach used in Ref. 7 and the component cost approach of Ref. 8. In our study, we define the following modal influence coefficient (MIC) and use it to rank the relative importance of the system's flexible modes.[4] Let us define the MIC using a simplified case with a single input and a single output, i.e., $a = m = 1$ in Eq. (5). Also, for simplicity, we have added a Rayleigh damping term $2\Delta_{nn}\Lambda^{1/2}_{nn}\dot{\xi}_n$ in Eq. (5). Let us denote $\Lambda_{nn} \triangleq \text{diag}(\omega^2_1, \omega^2_2, \ldots, \omega^2_i, \ldots)$, $\Delta_{nn} \triangleq \text{diag}(\zeta_1, \zeta_2, \ldots, \zeta_i, \ldots)$, $\Phi^T_{nn}G_{n1} \triangleq [g_1, g_2, \ldots, g_i, \ldots]^T$, and $H_{1n}\Phi_{nn} \triangleq [h_1, h_2, \ldots, h_i, \ldots]$, $i = 1, \ldots, n$. The transfer function from the input u_1 to the output y_1 is then given by

$$y_1(s)/u_1(s) = \sum_{i=1}^{i=n} g_ih_i/(s^2 + 2\zeta_i\omega_i s + \omega^2_i)$$

where s is a Laplace variable. The output response due to a unit step input can then be obtained by performing an inverse Laplace operation

$$y_1(t) = \mathcal{L}^{-1}\left[\sum_{i=1}^{i=n} g_ih_i/s(s^2 + 2\zeta_i\omega_i s + \omega^2_i)\right]$$
$$y_1(t) = \sum_{i=1}^{i=n} (g_ih_i/\omega^2_i)\left\{1 - e^{-\zeta_i\omega_i t}\cos\left[\omega_i\sqrt{1-\zeta^2_i}\,t - \tan^{-1}\left(\frac{\zeta_i}{\sqrt{1-\zeta^2_i}}\right)\right]\right\} \tag{7}$$

The system response is thus made up of n damped sinusoidal functions each at one system mode frequency. We call the amplitude of the sinusoidal function due to the ith mode, given by $|g_ih_i/\omega^2_i|$, its MIC. It is used in our study to rank and select system modes to be retained for subsequent projections. Rigid-body modes, with $\omega_i = 0$, are automatically retained.

In applying the P&A method on articulated, multiflexible body structures, we must decide which system modes are important and should be kept in Φ_{nk}. If the mode set Φ_{nk} contains only important modes from a particular (nominal) system configuration, our experience has indicated that the projected component models, when reassembled at other system configurations of interest, produce reduced-order system models that can miss important modes of these configurations. This is because the set of important system modes can change significantly with the system configurations.

To overcome this difficulty, a composite mode set, consisting of important system modes from all system configurations of interest, and not just from one particular configuration, can be used to advantage. With this understanding, we can perform the following projections [see Eqs. (3) and (6)]:

$$x^A_p \doteq P^A_{pn}\Phi_{nk}\xi^A_k \triangleq \Psi^A_{pk}\xi^A_k$$
$$x^B_q \doteq P^B_{qn}\Phi_{nk}\xi^B_k \triangleq \Psi^B_{qk}\xi^B_k \tag{8}$$

where ξ^A_k and ξ^B_k denote the reduced sets of generalized coordinates of component A and B, respectively. Substitutions of Eq. (8) into Eqs. (1) and (2) produce the constrained equations of motion of the components

$$\Psi^{A^T}_{pk}M^A_{pp}\Psi^A_{pk}\ddot{\xi}^A_k + \Psi^{A^T}_{pk}K^A_{pp}\Psi^a_{pk}\xi^A_k = \Psi^{A^T}_{pk}G^A_{pa}u^A_a$$
$$\Psi^{B^T}_{qk}M^B_{qq}\Psi^B_{qk}\ddot{\xi}^B_k + \Psi^{B^T}_{qk}K^B_{qq}\Psi^B_{qk}\xi^B_k = \Psi^{B^T}_{qk}G^B_{qa}u^B_a \tag{9}$$

Implicit in Eqs. (8) and (9) are the assumptions that both Ψ^A_{pk} and Ψ^B_{qk} are of full column rank. These assumptions are violated when k is greater than either p or q. Situations may also arise when the projected component modes are linearly dependent on each other. When the Ritz transformation matrices Ψ^A_{pk} and Ψ^B_{qk} are rank deficient, a singular value decom-

position (SVD) technique can be used to find orthogonal sets of vectors spanning their rank spaces. In effect, dependent columns in Ψ^A_{pk} and Ψ^B_{qK} are eliminated.[3,5]

Let the I/F compatibility relations between the components be represented by $C^A_{ip}(\alpha)x^A_p + C^B_{iq}(\alpha)x^B_q = O_i$. Here, C^A_{ip} and C^B_{iq} are matrices that establish the constraint relations between components A and B. The last equation can also be rewritten as [see Eq. (8)]

$$[C^A_{ip}\Psi^A_{pk} \quad C^B_{iq}\Psi^B_{qk}]\begin{bmatrix}\xi^A_k\\ \xi^B_k\end{bmatrix} \triangleq [D_{ij}]\begin{bmatrix}\xi^A_k\\ \xi^B_k\end{bmatrix} \doteq O_i \tag{10}$$

where $j = 2k$. To construct the reduced-order system model, we partition the compatibility matrix D_{ij} using the SVD technique

$$[D_{ij}] = [U_{ii}][\Sigma_{ii}, O_{is}]\begin{bmatrix}P^T_{ji}\\ P^T_{js}\end{bmatrix} \tag{11}$$

where $s = j - i$, Σ_{ii} is an $i \times i$ diagonal matrix with the i singular values of the matrix D_{ij} along its diagonal, and O_{is} is an $i \times s$ null matrix. The partitioned matrix P_{js} in Eq. (11) can be used as follows[3,6]:

$$\begin{bmatrix}\xi^A_k\\ \xi^B_k\end{bmatrix} = [P_{js}]\xi_s \triangleq \begin{bmatrix}P^A_{ks}\\ P^B_{ks}\end{bmatrix}\xi_s \tag{12}$$

Substituting $\xi^A_k = P^A_{ks}\xi_s$ and $\xi^B_k = P^B_{ks}\xi_s$ into Eq. (9), premultiplying the resultant equations by $P^{A^T}_{ks}$ and $P^{B^T}_{ks}$, respectively, and summing the resultant equations give

$$\begin{aligned} M_{ss}\ddot{\xi}_s + K_{ss}\xi_s &= G_{sa}u_a \\ y_m &= H_{ms}\xi_s \end{aligned} \tag{13}$$

where $M_{ss} = P^{A^T}_{ks}\Psi^{A^T}_{pk}M^A_{pp}\Psi^A_{pk}P^A_{ks} + P^{B^T}_{ks}\Psi^{B^T}_{qk}M^B_{qq}\Psi^B_{qk}P^B_{ks}$. Similar expressions can also be written for K_{ss}, etc. Let $(\Phi_{ss}, \Lambda_{ss}) = \text{eig}(K_{ss}, M_{ss})$, the modal equivalence of Eq. (13) is

$$\begin{aligned} I_{ss}\ddot{\eta}_s + \Lambda_{ss}\eta_s &= \Phi^T_{ss}G_{sa}u_a \\ y_m &= H_{ms}\Phi_{ss}\eta_s \end{aligned} \tag{14}$$

where η_s is the modal coordinate, i.e., $\xi_s = \Phi_{ss}\eta_s$. Also, $\Phi^T_{ss}M_{ss}\Phi_{ss} = I_{ss}$, and $\Lambda_{ss} = \Phi^T_{ss}K_{ss}\Phi_{ss}$ is a diagonal matrix with the undamped, reduced-order system eigenvalues along its diagonal. It has been proven that Φ_{nk} is captured exactly in Φ_{ss}, together with a number of extraneous modes.[3,5] Hence, Λ_{ss} and Φ_{ss} can be expressed as

$$\Lambda_{ss} \triangleq \begin{bmatrix}\Lambda_{kk} & O_{ke}\\ O_{ek} & \Lambda_{ee}\end{bmatrix} \tag{15}$$

$$\Phi_{ss} \triangleq [\Phi_{sk} \ \Phi_{se}] \tag{16}$$

where the eigenvector matrices Φ_{sk} and Φ_{se} are for the kept and extraneous modes, respectively, and Λ_{kk} and Λ_{ee} are the corresponding eigenvalue matrices.

Static Gains of the Full- and Reduced-Order Systems

As was pointed out in Ref. 6, the P&A method, although capturing the system's modes of interest exactly, does not preserve its static gain. With reference to Ref. 6, the static gain of the full-order system, from the control input u_a to the output y_m, is given by

$$E^F_{ma} = H_{mn}(\Phi_{nk}\Lambda^{-1}_{kk}\Phi^T_{nk} + \Phi_{nt}\Lambda^{-1}_{tt}\Phi^T_{nt})G_{na} \tag{17}$$

where Λ_{kk} and Λ_{tt} are the kept and truncated eigenvalue matrices, respectively [see Eq. (6)], and E^F_{ma} is a $m \times a$ static gain matrix. We have assumed here that the inverses of both Λ_{kk} and Λ_{tt} exist (i.e., the system does not contain any rigid-body modes). If the system contains rigid-body modes, a pseudostatic gain, containing only contributions from the system's flexible modes, can be defined by first removing the rigid-body modes from Λ_{kk}

$$\Phi_{nk} \triangleq [\Phi_{nr} \quad \Phi_{nf}], \qquad \Lambda_{kk} \triangleq \begin{bmatrix}O_{rr} & O_{rf}\\ O_{fr} & \Lambda_{ff}\end{bmatrix} \tag{18}$$

where Φ_{nr} and Φ_{nf} are eigenvectors associated with the rigid-body and flexible modes, respectively. The matrix Λ_{ff} contains eigenvalues associated with the kept flexible modes. The pseudostatic gain is defined as

$$\bar{E}^F_{ma} = H_{mn}(\Phi_{nf}\Lambda^{-1}_{ff}\Phi^T_{nf} + \Phi_{nt}\Lambda^{-1}_{tt}\Phi^T_{nt})G_{na} \tag{19}$$

Similarly, the static gain and pseudostatic gain of the reduced-order system model are[6]

$$E^R_{ma} = H_{mn}(\Phi_{nk}\Lambda^{-1}_{kk}\Phi^T_{nk} + \Phi_{ne}\Lambda^{-1}_{ee}\Phi^T_{ne})G_{na} \tag{20}$$

$$\bar{E}^R_{ma} = H_{mn}(\Phi_{nf}\Lambda^{-1}_{ff}\Phi^T_{nf} + \Phi_{ne}\Lambda^{-1}_{ee}\Phi^T_{ne})G_{na} \tag{21}$$

The matrix Φ_{ne} used in Eqs. (20) and (21) was defined in Ref. 6. Comparing Eq. (17) with Eq. (20) [or Eq. (19) with Eq. (21)], we note that $E^F_{ma} \neq E^R_{ma}$ since $\Phi_{nt}\Lambda^{-1}_{tt}\Phi^T_{nt} \neq \Phi_{ne}\Lambda^{-1}_{ee}\Phi^T_{ne}$ in general. Hence the static gain of the full-order system at the nominal configuration, or at any other configuration, is not preserved in the reduced-order system model.

Enhanced Projection and Assembly (EP&A) Methodology

Two different approaches were introduced in Ref. 6 to preserve the static gain of the full-order model in the reduced-order model. These approaches are illustrated in Fig. 2. The first approach involves augmenting the k kept modes of the system with additional a modes (a is the number of control inputs) so as to create a statically complete mode set. The augmented mode set is then projected onto the components, and the reduced component models are reassembled as usual. In the second approach, the k kept modes of the system are first projected onto the components. The reduced component mode sets are then each augmented with static correction modes. The details of these approaches are given later.

System Level Augmentation

The system modal equation (5) can be decomposed into its kept and truncated parts

$$I_{kk}\ddot{\xi}_k + \Lambda_{kk}\xi_k = \Phi^T_{nk}G_{na}u_a \tag{22}$$

$$I_{tt}\ddot{\xi}_t + \Lambda_{tt}\xi_t = \Phi^T_{nt}G_{na}u_a \tag{23}$$

The static effects of the truncated mode set Φ_{nt} due to control inputs can be approximated by a smaller but statically equivalent mode set Φ_{na}. To find Φ_{na}, consider the following Ritz transformation:

$$\xi_t = R_{ta}\xi_a \triangleq [\Lambda^{-1}_{tt}\Phi^T_{nt}G_{na}]\xi_a \tag{24}$$

Here ξ_a is the generalized coordinate associated with the augmented mode set Φ_{na}. Substituting of Eq. (24) into Eq. (23), and premultiplying the result by y/R^T_{ta} give

$$R^T_{ta}R_{ta}\ddot{\xi}_a + R^T_{ta}\Lambda_{tt}R_{ta}\xi_a = R^T_{ta}\Phi^T_{nt}G_{na}u_a \tag{25}$$

The contribution of ξ_a in the static gain of the reduced-order model is

$$\begin{aligned} E^R_{ma}(\text{due to } \xi_a) &= H_{mn}\Phi_{nt}R_{ta}(R^T_{ta}\Lambda_{tt}R_{ta})^{-1}R^T_{ta}\Phi^T_{nt}G_{na} \\ &= H_{mm}\Phi_{nt}\Lambda^{-1}_{tt}\Phi^T_{nt}G_{na} \end{aligned} \tag{26}$$

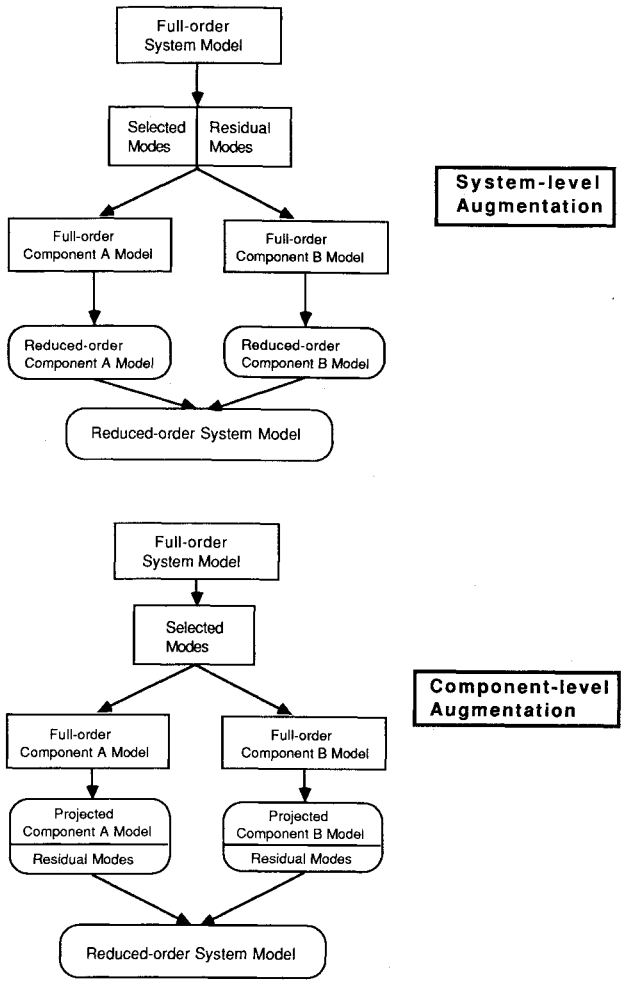

Fig. 2 Graphical illustrations of the EP&A model reduction approaches.

where the second equation was obtained using Eq. (24). The static gain due to the mode set $[\Phi_{nk}\ \Phi_{na}] = [\Phi_{nk}\Phi_{nt}R_{ta}]$ is thus identical to that of the full-order model [see Eq. (17)]. Hence, $[\Phi_{nk}\Phi_{nt}R_{ta}]$ is a statically complete mode set. This mode set is then projected onto the flexible component models to generate reduced-order component models (see Fig. 2). In spite of this augmentation, the selected mode set Φ_{nk} is still exactly captured in the reduced-order system model.[6]

Component-Level Augmentation

In this approach, the k kept modes are first projected onto the components. From Eq. (8), we have

$$x_p^A = \Psi_{pk}^A \Xi_{kk}^A \eta_k^A \triangleq \Upsilon_{pk}^A \eta_k^A \triangleq [\Upsilon_{pr}^A \Upsilon_{pf}^A]\eta_k^A$$
$$x_q^B = \Psi_{qk}^B \Xi_{kk}^B \eta_k^B \triangleq \Upsilon_{qk}^B \eta_k^B \triangleq [\Upsilon_{qr}^B \Upsilon_{qf}^B]\eta_k^B \tag{27}$$

Here, Ξ_{kk}^A and Ξ_{kk}^B are the eigenvector matrices associated with the eigenvalue problems of the first and second equations of Eq. (9), respectively, and $\xi_k^A = \Xi_{kk}^A \eta_k^A$ and $\xi_k^B = \Xi_{kk}^B \eta_k^B$. Matrix partitions Υ_{pr}^A and Υ_{pf}^A denote eigenvectors associated with the rigid-body and flexible modes of the projected component A model. Similar partitions can also be made for component B. Let Υ_{pr}^A, Υ_{pf}^A, etc., be normalized such that

$$\Upsilon_{pr}^{A^T} M_{pp}^A \Upsilon_{pr}^A = I_{rr}, \qquad \Upsilon_{pr}^{A^T} K_{pp}^A \Upsilon_{pr}^A = O_{rr}$$
$$\Upsilon_{pf}^{A^T} M_{pp}^A \Upsilon_{pf}^A = I_{ff}, \qquad \Upsilon_{pf}^{A^T} K_{pp}^A \Upsilon_{pf}^A = \Lambda_{ff}^A \tag{28}$$

where Λ_{ff}^A is the eigenvalue matrix associated with the flexible modes of the projected component A model. Using the matrices defined in Eq. (27) and (28), residual inertia-relief attachment modes[9,10] (called residual modes in the sequel) can be generated to augment the projected mode sets of the components. For component A, the residual modes are given by

$$\Upsilon_{pa}^A = (\bar{P}_{pp}^{A^T} \bar{S}_{pp}^A \bar{P}_{pp}^A - \Upsilon_{pf}^A \Lambda_{ff}^{A^{-1}} \Upsilon_{pf}^{A^T}) F_{pa}^A \tag{29}$$

where $\bar{P}_{pp}^A = I_{pp}^A - M_{pp}^A \Upsilon_{pr}^A \Upsilon_{pr}^{A^T}$, and $\bar{S}_{pp}^A$ is the pseudoflexibility matrix of the component A. The pseudoflexibility matrix is defined as follows. Let the set $\bar{p}$ of all physical coordinates be divided into three sets: $\bar{c}$, $\bar{a}$, and $\bar{w}$. The $\bar{c}$ set may be any statically determinate constraint set that provides restraint against rigid-body motion. The $\bar{a}$ set consists of coordinates where unit forces are to be applied to define attachment modes (e.g., at the interface coordinates and at coordinates where external forces are applied). The $\bar{w}$ set consists of the remaining coordinates in $\bar{p}$. Using these definitions, the stiffness matrix of component A, K_{pp}^A, is partitioned as follows:

$$\begin{bmatrix} k_{ww} & k_{wa} & k_{wc} \\ k_{aw} & k_{aa} & k_{ac} \\ k_{cw} & k_{ca} & k_{cc} \end{bmatrix} \tag{30}$$

The pseudoflexibility matrix $\bar{S}_{pp}^A$ for component A is

$$\begin{bmatrix} \begin{bmatrix} k_{ww} & k_{wa} \\ k_{aw} & k_{aa} \end{bmatrix}^{-1} & \begin{matrix} 0 \\ 0 \end{matrix} \\ \begin{matrix} 0 & 0 \end{matrix} & 0 \end{bmatrix} \tag{31}$$

In Eq. (29), the matrix F_{pa}^A is given by $[O_{aw}, I_{aa}, O_{ac}]^T$, where the identity matrix I_{aa} is associated with the $\bar{a}$ set. Similar expressions can also be written for component B.

The projected mode sets Υ_{pk}^A and Υ_{qk}^B can now be augmented with the residual modes

$$x_p^A = [\Upsilon_{pk}^A \Upsilon_{pa}^A] \begin{bmatrix} \eta_k^A \\ \eta_a^A \end{bmatrix} \triangleq \Upsilon_{pv}^A \nu_v^A$$
$$x_q^B = [\Upsilon_{qk}^B \Upsilon_{qa}^B] \begin{bmatrix} \eta_k^B \\ \eta_a^B \end{bmatrix} \triangleq \Upsilon_{qv}^B \nu_v^B \tag{32}$$

where η_a^A and η_a^B are generalized coordinates associated with the residual modes, and $v = k + a$. Using Eqs. (32), the equations of motion of the projected component models are

$$\Upsilon_{pv}^{A^T} M_{pp}^A \Upsilon_{pv}^A \ddot{\nu}_v^A + \Upsilon_{pv}^{A^T} K_{pp}^A \Upsilon_{pv}^A \nu_v^A = \Upsilon_{pv}^{A^T} G_{pa}^A u_a$$
$$\Upsilon_{qv}^{B^T} M_{qq}^B \Upsilon_{qv}^B \ddot{\nu}_v^B + \Upsilon_{qv}^{B^T} K_{qq}^B \Upsilon_{qv}^B \nu_v^B = \Upsilon_{qv}^{B^T} G_{qa}^B u_a \tag{33}$$

These reduced-order component models are then combined using the I/F compatibility relations to generate the reduced-order system model. The steps involved are similar to those described by Eqs. (10–13), and will not be repeated here.

Applications on the Galileo Cruise Model

The effectiveness of the EP&A method will now be demonstrated using a high-order finite element model of the Galileo dual-spin spacecraft. Figure 1 depicts the three-body topology of the spacecraft. The rotor is the largest and most flexible component represented with 243 dynamic DOFs. The smaller and more rigid stator is represented with 57 dynamic DOFs. Lastly, the scan platform is the smallest body idealized as rigid with 6 DOFs.

For the purpose of controller design, low-order system models, accurate at all system configurations of interest and over a frequency range of 0–10 Hz, are needed. To this end, the MIC criterion is used to select important system modes from six system configurations with clock angles of 0, 60, 120, 180, 240, and 300 deg. A composite mode set is then constructed that encompasses all the important modes at these

system configurations. The composite mode set has 28 modes, which includes 8 rigid-body modes.

Using the P&A method, the composite mode set is projected onto both the rotor and stator models. The projection was performed at the 300-deg clock angle since previous studies indicated that the clock controller has the smallest gain margin at this clock angle. Two rigid-body modes, one describing the stator articulation and the other describing the platform articulation, were eliminated from the reduced-order rotor mode set since they are not rigid-body modes of the rotor. Also, not all projected modes of the stator are independent, and an SVD technique was used to eliminate the dependent modes. This resulted in 19 modes being projected for the stator (eight rigid-body and 11 flexible modes) and 26 modes being projected for the rotor (six rigid-body and 20 flexible modes).

The reduced rotor and stator models and the rigid scan platform were then assembled to generate the reduced-order system models. Six constraints exist between the rotor and the stator, and six between the stator and the scan platform. As such, the assembled system model has 39 DOF ($26 + 19 + 6 - 6 - 6 = 39$). Out of these 39 modes, eight are rigid-body modes, 11 are extraneous modes, and the remaining 20 are the selected modes, which have been captured exactly.

A comparison of the Bode plots of the full-order and reduced-order Galileo models at a clock angle of 300 deg is given in Fig. 3. Actuation was done at the spin bearing assembly, located at the rotor-stator interface (along the Z axis), and sensing done by a gyroscope located at the scan platform (see Fig. 1). In Fig. 3, as well as in all subsequent Bode plots, we have assumed a uniform 0.25% modal damping factor for all the system's modes. Also, the contributions of all modes with

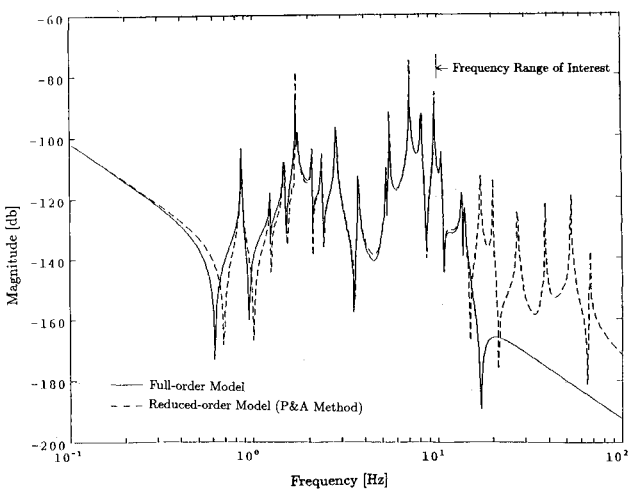

Fig. 3 Bode plot comparison, P&A method at 300 deg.

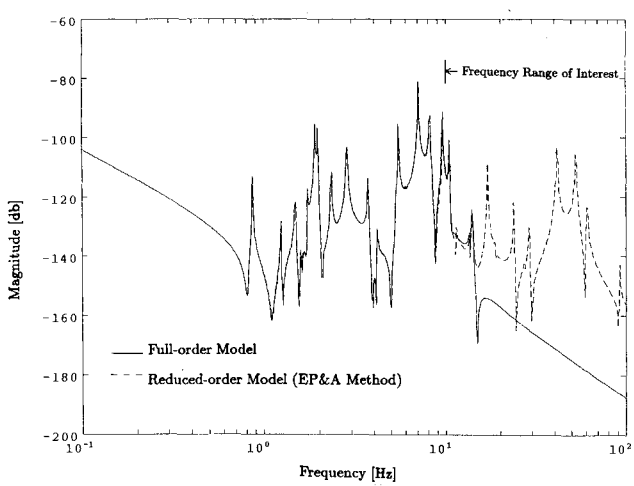

Fig. 4 Bode plot comparison, EP&A method at 0 deg.

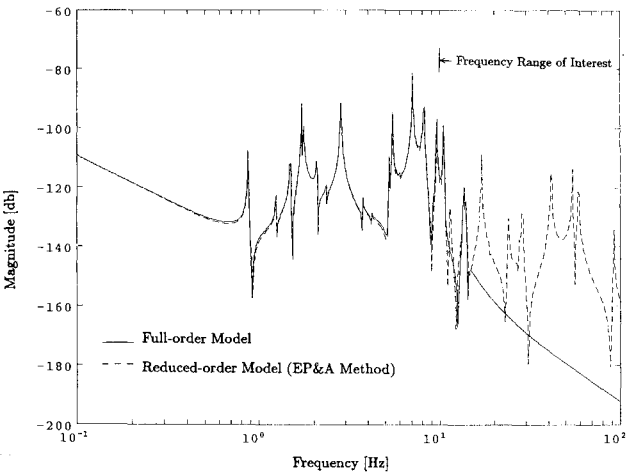

Fig. 5 Bode plot comparison, EP&A method at 60 deg.

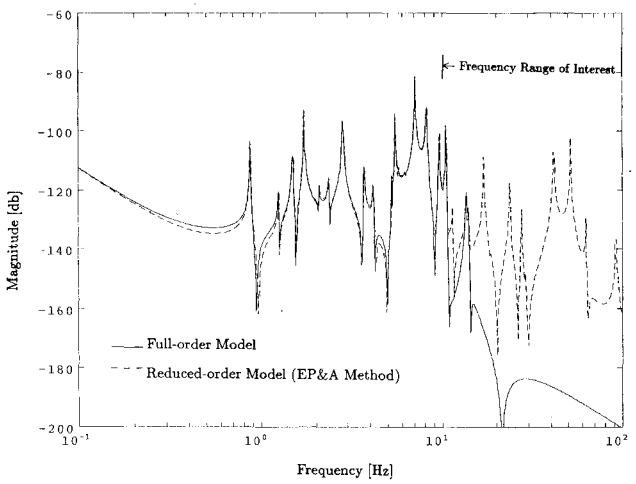

Fig. 6 Bode plot comparison, EP&A method at 120 deg.

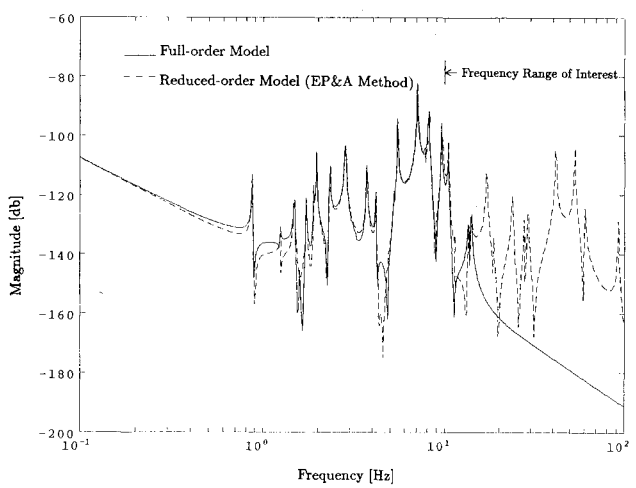

Fig. 7 Bode plot comparison, EP&A method at 180 deg.

frequencies greater than 20 Hz in the full-order Bode plots have been removed to expose the extraneous modes of the reduced-order model. Bode plot comparisons at other clock angles are not given here to save space. At the projection configuration (300 deg), the selected modes of interest have been captured exactly, but there are significant mismatches of low-frequency zeros between the full-order and reduced-order models. Results obtained at other system configurations (not given) revealed similar mismatches.

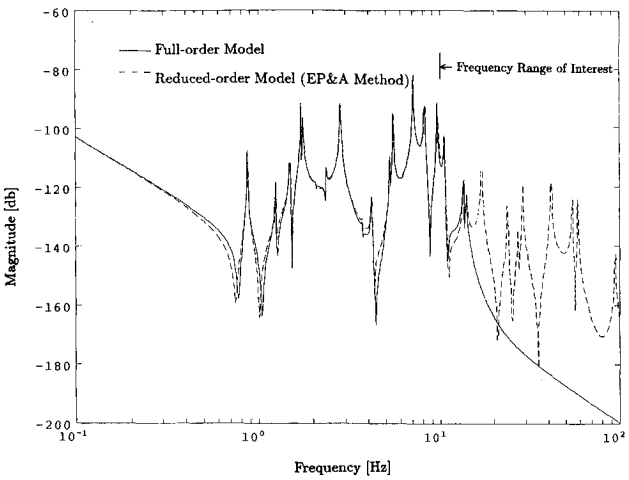

Fig. 8 Bode plot comparison, EP&A method at 240 deg.

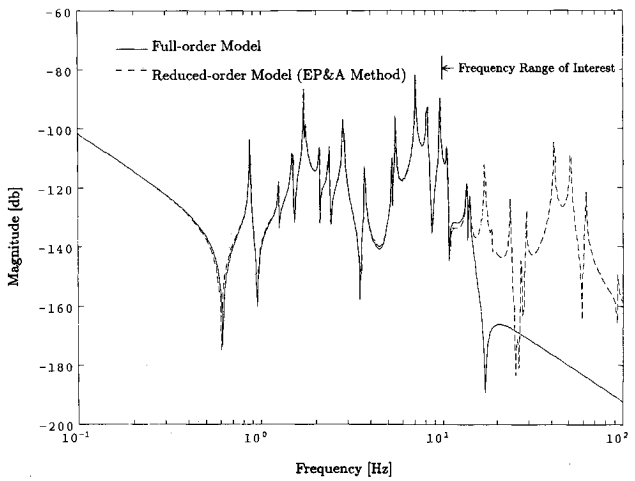

Fig. 9 Bode plot comparison, EP&A method at 300 deg.

Table 1 Pseudostatic gains of the full- and reduced-order Galileo models (rad/Nm)

α, deg	$E^F \times 10^7$ (full)	$E^R \times 10^7$ (EP&A)	$E^F \times 10^7$ (P&A)
0	26.125	26.084	4.985
60	14.572	14.718	7.947
120	−5.564	−5.101	−3.162
180	14.928	15.473	4.011
240	9.849	10.270	4.769
300	1.746	1.897	6.712

The system-level EP&A method was then applied to the Galileo model. The original composite mode set of the system was augmented with two residual modes, one for an input torque about the Z axis on the rotor side of the rotor/stator interface and a second equal and opposite torque on the stator side of the interface. The enlarged mode set was then projected onto the components, and an SVD was used to remove linearly dependent modes. The resultant reduced-order models of the rotor, stator, and scan platform have 28, 21, and 6 modes, respectively. The assembled reduced-order model has 43 modes (28 + 21 + 6 − 6 − 6 = 43). Of these 43 modes, 8 are rigid-body modes, 20 are selected system modes, and 15 are extraneous modes.

Comparisons of Bode plots of the full-order and reduced-order models obtained using the EP&A method, at clock angles of 0, 60, 120, 180, 240, and 300 deg, are given in Figs. 4–9, respectively. Once again, we observe that the selected modes of interest have been captured exactly at the projection configuration (see Fig. 9). Moreover, the mismatches between the zeros of the full-order model and reduced-order model we witnessed in Fig. 3 have been significantly reduced. Similar improved matchings are also observed at other system configurations (see Figs. 4–8). Expectedly, the pseudostatic gains of the reduced-order system models produced by the EP&A method, at all clock angles studied, are closer to their full-order counterparts than those produced by the P&A method (see Table 1).

Concluding Remarks

To apply the P&A method on structures with articulated flexible bodies, a composite mode set, consisting of important modes from all system configurations of interest and not just from one particular configuration, can be used to advantage. However, this task is not easy because it is difficult to establish a common yardstick to measure the relative importance of system modes across the various system configurations of interest. The selected mode set is at best a good guess. Inevitably, modes that contribute significantly to system behavior at some configurations may be missed.

To approximate the contributions of high-frequency modes neglected by the use of a truncated eigenbasis, we propose to augment the composite mode set with residual mode(s), at either the system or component level, before the mode set is projected on the component models. The proposed method is called an EP&A model reduction methodology. Results obtained with a high-order, finite element model of the Galileo spacecraft, using a system-level augmentation approach are given here, and those found using the component-level augmentation are given in Ref. 11. These results demonstrated the effectiveness of the EP&A methodology in generating reduced-order system models that closely match those of the full-order models, over a frequency range of interest, at all system configurations of interest.

To generate the composite mode set used in the EP&A methodology, we must solve a large-order eigenvalue problem repetitively. This is a drawback. To circumvent this difficulty, we have proposed in Ref. 12 an approach in which component modes such as the Craig-Bampton mode sets[9] are first used to reduce the full-order component models. The resultant component models are then combined to generate a reduced-order system model. Typically, the size of this system model is still too large for multibody dynamic simulation, and the EP&A methodology can then be used to reduce it further. Results obtained are given in Ref. 12.

Since the reduced-order models will ultimately be used for nonlinear simulations, the final comparison between the full- and reduced-order models should be done in the time domain. However, judging by the fact that the reduced-order system models closely reproduced the frequency responses of their full-order counterparts at the various system configurations, we expect to obtain good time domain results with this approach if the articulation rate is sufficiently slow. However, this must be confirmed and quantified via careful nonlinear, time simulations. The effects that increasing slew rate has on the effectiveness of the methodology is an interesting topic to pursue in the future.

Acknowledgments

The research described in this paper was conducted at the Jet Propulsion Laboratory, California Institute of Technology, under a contract with NASA. The authors wish to thank their colleagues at JPL, including F. Hadaegh, G. Macala, J. Spanos, and M. Wette for many helpful discussions and valuable suggestions. We also wish to thank M. Lou and G. Man for their interest and encouragement. All errors are our responsibility.

References

[1]Bodley, C. S., Devers, A. D., Park, A. C., and Frisch, H. P., "A Digital Computer Program for the Dynamic Interaction Simulation of Controls and Structure (DISCOS)," NASA Center for Aerospace

Information, NASA TP1219, Vols. I and II, Baltimore, MD, May 1978.

[2]Spanos, J. T., and Tsuha, W., "Selection of Component Modes for the Simulation of Flexible Multibody Spacecraft," *Journal of Guidance, Control, and Dynamics,* Vol. 14, No. 2, 1991, pp. 278–286.

[3]Bernard, D., "Projection and Assembly Method for Multibody Component Model Reduction," *Journal of Guidance, Control, and Dynamics,* Vol. 13, No. 5, 1990, pp. 905–912.

[4]Eke, F. O., and Man, G. K., "Model Reduction in the Simulation of Interconnected Flexible Bodies," *Proceedings of the AAS/AIAA Astrodynamics Specialist Conference*, Part 1, 1987, pp. 603–612 (AAS Paper 87-455).

[5]Tsuha, W., and Spanos, J. T., "Reduced Order Component Modes for Flexible Multibody Dynamics Simulations," AIAA Aerospace Sciences Meeting, AIAA Paper 90-0662, Reno, NV, Jan. 1990.

[6]Lee, A. Y., and Tsuha, W. S., "An Enhanced Projection and Assembly Model Reduction Methodology," *Proceedings of the AIAA Guidance, Navigation, and Control Conference* (New Orleans), AIAA, Washington, DC, 1991, pp. 1350–1359 (AIAA Paper 91-2749).

[7]Gregory, C. Z., "Reduction of Large Flexible Spacecraft Models Using Internal Balancing Theory," *Journal of Guidance, Control, and Dynamics,* Vol. 7, No. 6, 1984, pp. 725-732.

[8]Skelton, R. E., Singh, R., and Ramakrishnan, J., "Component Model Reduction by Component Cost Analysis," AIAA Paper 88-4086, Aug. 1988.

[9]Craig, R. R., Jr., *Structural Dynamics: An Introduction to Computer Methods,* Wiley, New York, 1981.

[10]Craig, R. R., Jr., and Chang, C. J., "On the Use of Attachment Modes in Substructure Coupling for Dynamic Analysis," *Proceedings of the AIAA/ASME 18th Structures, Structural Dynamics, and Material Conference,* Vol. B, AIAA, New York, 1977, pp. 89–99 (AIAA Paper 77-405).

[11]Lee, A. Y., and Tsuha, W. S., "An Enhanced Projection and Assembly Model Reduction Methodology," Jet Propulsion Lab., California Inst. of Technology, JPL Internal Document D-7773, Pasadena, CA, Sept. 1990.

[12]Lee, A. Y., and Tsuha, W. S., "A Component Modes Projection and Assembly Model Reduction Methodology for Articulated Flexible Structures," *Proceedings of the AIAA Guidance, Navigation, and Control Conference* (Hilton Head, SC), AIAA, Washington, DC, 1992, pp. 143–153 (AIAA Paper 92-4323).